Energy Harvesting Enabled NOMA Systems with Full-duplex Relaying

Cheng Guo, Liqiang Zhao, *Member, IEEE*, Chen Feng, *Member, IEEE*, Zhiguo Ding, *Senior Member, IEEE*, and Hsiao-Hwa Chen, *Fellow, IEEE*

***Abstract*—This paper investigates an integrated wireless communication system including non-orthogonal multiple access, full-duplex relaying, and energy harvesting techniques (named as EH-FD-NOMA). In this scheme, an energy-limited full-duplex relay harvests energy from a source at the first stage. Then, the relay detects the superimposed signal from the source and transmits the decoded signal to destination. Closed-form outage probabilities and ergodic rates at the relay and destination are derived. Numerical results verify the analytical results and show the superior performance of the EH-FD-NOMA if compared to its counterparts.**

***Index Terms*—Energy harvesting; NOMA; Full-duplex; Ergodic rate; Fairness; Outage probability.**

I. INTRODUCTION

Rapid growth in wireless communications pushes for a significantly improved spectrum efficiency (SE) in the future wireless networks. Non-orthogonal multiple access (NOMA) was proposed to provide an extra domain to separate users on the same resource block to detect the superimposed users using successive interference cancellation (SIC) [1].

To enhance the performance of NOMA, [2] proposed a cooperative NOMA, in which nearby NOMA users detect signals of far-away NOMA users and act as relays to assist the far-away users for reliable communications. The results indicated that the cooperative NOMA offers a better performance than conventional NOMA. Although cooperative NOMA can offer a performance gain, it leads to an extra bandwidth loss. To deal with this issue, a full-duplex (FD) relay transmitting and receiving messages on the same frequency channel simultaneously can be used to double SE [3].

This paper was submitted on October 17, 2018, and revised on April 29, 2019. The work of L. Zhao and C. Guo was supported by the National Natural Science Foundation of China (61771358), National Natural Science Foundation of Shaanxi Province (2018JM6052), and the 111 Project (B08038). The work of C. Feng was supported by the NSERC Discovery Grants RGPIN-2016-05310. The work of Z. Ding was supported by the UK EPSRC under grant number EP/N005597/2, NSFC under grant number 61728101 and H2020-MSCA-RISE-2015 under grant number 690750.

Cheng Guo (e-mail: guoch@stu.xidian.edu.cn) and Liqiang Zhao (e-mail: lqzhao@mail.xidian.edu.cn) are with the State Key Laboratory of Integrated Service Networks, Xidian University, China. Chen Feng (e-mail: chen.feng@ubc.ca) is with the School of Engineering, the University of British Columbia, Canada. Zhiguo Ding (e-mail: zhiguo.ding@manchester.ac.uk) is with the School of Electrical and Electronic Engineering, the University of Manchester, UK. Hsiao-Hwa Chen (e-mail: hshwchen@ieee.org) is with the Department of Engineering Science, National Cheng Kung University, Taiwan. (*Corresponding author: Hsiao-Hwa Chen*)

In addition to SE improvement, it is also important to prolong the lifetime of wireless nodes, especially in energy-limited applications. To tackle the energy-limited problem, energy harvesting (EH) is an effective method to provide additional lifespan of wireless nodes. Simultaneous wireless information and power transfer (SWIPT) was investigated first in [4] as an EH method working on radio frequency, which is not a practical receiver architecture. In order to make use of SWIPT in practice, [5] proposed two SWIPT schemes, namely time switching (TS) and power splitting (PS).

There have been numerous works on the combination of cooperative NOMA with SWIPT. [6] proposed a SWIPT enabled cooperative NOMA scheme, where far-away NOMA users are assisted by nearby NOMA users acting as EH relays, and the outage probability and throughput were analyzed. In [7], a SWIPT aided cooperative NOMA system with multiple antennas at BS was proposed and a joint optimization of beamforming and PS was achieved. [8] considered a SWIPT assisted cooperative NOMA system, studied the issues of power allocation, and derived the outage probability of a network. [9] derived an approximate outage probability of two users and proposed a user-paring method for a cooperative NOMA system with SWIPT. In [10], the authors applied SWIPT to a cooperative NOMA system and optimized power allocation and PS coefficients by maximizing energy efficiency. [11] investigated a far-away NOMA user's outage probability and diversity order for an multiple-input single-output (MISO) cooperative NOMA network with hybrid SWIPT. [12] applied SWIPT to an MISO cooperative NOMA network and optimized beamforming and PS coefficient by maximizing a nearby user's rate with a far-away user's QoS constraint. The authors of [13] analyzed the outage probability and system throughput for a cooperative NOMA network with SWIPT and discussed the impact of PS scheme on the performance of two users. [14] studied the outage probability and diversity order with two different antenna selection methods in an MISO cooperative NOMA system.

In addition, the integration of cooperative NOMA and FD was also investigated in the literature. [15] considered a cooperative NOMA network with FD relaying, for which system outage probability and ergodic rate were derived. [16] proposed a NOMA with FD relaying network and analyzed its performance. [17] characterized the outage probabilities, user data rates and energy efficiency in a cooperative NOMA network with FD relaying. The authors in [18] applied FD technology to a cooperative NOMA system and analyzed the outage probabilities of nearby and far-away users. [19]

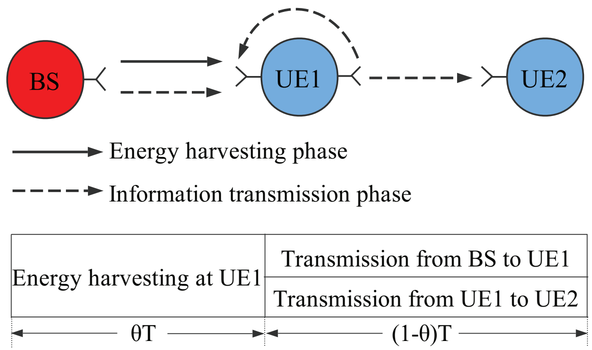

Fig. 1. System model of EH-FD-NOMA and illustration of the TS protocol.

presented a cooperative NOMA network with FD relaying and analyzed the outage probability for a far-away user. In [20], the authors characterized the outage probability and ergodic rate in a cooperative NOMA network with AF FD relaying. [21] derived the outage probability and ergodic sum rate for a FD cooperative NOMA network considering different antenna selection schemes. In [22], the authors derived outage probability and diversity orders, employing a single-stage relay selection scheme in a FD aided cooperative NOMA network.

However, to the best of our knowledge, there is still a lack of theoretical analysis on the performance of the EH-FD-NOMA systems. This work focuses on an EH-FD-NOMA system, where EH can be viewed as an effective way to inspire the cooperation when a relay node is energy-limited. Numerical results verify the analytical solutions, showing the superiority of the EH-FD-NOMA system in terms of outage probability, ergodic rate, and fairness.

II. SYSTEM MODEL

Let us consider a wireless network consisting of one BS and two users, namely UE1 and UE2, as shown in Fig. 1. The BS transmits information to UE2 with the aid of UE1, which is an EH FD relay node. The BS and UE2 have only one antenna. UE1 has two antennas, in which one antenna used only for EH and information reception, and the other used only for information transmission. There is no direct link from the BS to UE2 because of shadowing and long propagation distance. Assume that UE1 is an energy-limited node, whose operation relies on the harvested energy from the BS. Let h_{sr} denote the channel coefficient from BS to UE1, and h_{rd} is the channel coefficient between UE1 and UE2, respectively. Assume that h_{sr} and h_{rd} are independent Rayleigh fading coefficients. Thus, the channel power gains $|h_{sr}|^2$ and $|h_{rd}|^2$ can be viewed as exponentially distributed random variables with means λ_{sr} and λ_{rd}, respectively.

Moreover, assume that the TS protocol is used in this EH system. Hence, the entire communication process consists of EH phase and information transmission phase. θT is employed in the EH phase at UE1, and $(1-\theta)T$ is employed in the information transmission phase, where T is the entire transmission time and $\theta \in (0,1)$ is a system parameter.

The BS transmits superimposed signals based on the NOMA principle, or

$$x(t) = \sqrt{aP_t}x_1(t) + \sqrt{(1-a)P_t}x_2(t), \tag{1}$$

where P_t denotes the transmission power of the BS, and $a \in (0, 0.5)$ is the power allocation coefficient for UE1 (similarly, $1-a$ denotes the coefficient for UE2). Note that the constraint $0 < a < 0.5$ comes from the NOMA principle, which specifies that more power should be allocated to UE2 than UE1. Here, x_1 and x_2 are the transmitted signals for UE1 and UE2 with $\mathbb{E}\{|x_1|^2\} = \mathbb{E}\{|x_2|^2\} = 1$. Next, let us explain EH phase and information transmission phase as follows.

1) In the EH phase, the received signal at UE1 is given by

$$y_r(t_1) = \frac{h_{sr}}{\sqrt{d_{sr}^{\alpha}}}x(t_1) + n_r(t_1), \tag{2}$$

where h_{sr} captures the small-scale fading effect, d_{sr}^{α} denotes the large-scale fading effect, and n_r is zero mean additive white Gaussian noise (AWGN) with variance N_0.
Assume that UE1 uses total harvested energy to relay its detected message of UE2. The harvested energy is given by

$$E = \frac{\eta |h_{sr}|^2 P_t}{d_{sr}^{\alpha}}\theta T, \tag{3}$$

where η denotes energy conversion efficiency.
Hence, the transmit power at UE1 can be expressed as

$$P_r = \frac{\eta |h_{sr}|^2 P_t \theta}{d_{sr}^{\alpha}(1-\theta)}. \tag{4}$$

2) In the information transmission phase, assume that UE1 cannot remove self interference of FD relaying completely. Thus, UE1 may receive two signals simultaneously, including the superimposed message of the BS and self interference of FD. The received signal of UE1 is

$$y_r(t_2) = \frac{h_{sr}}{\sqrt{d_{sr}^{\alpha}}}x(t_2) + \sqrt{I_s}x_2(t_2-\delta) + n_r(t_2), \tag{5}$$

where I_s is the self-interference power and δ is a processing delay, as UE1 needs time to harvest energy from BS and employs SIC for information decoding. The delay could not be ignored if compared to the entire transmission time.

After UE1 receives y_r, it decodes x_2 first and subtracts this component from y_r for decoding x_1 itself in the process of SIC. Hence, the signal to interference and noise ratio (SINR) of UE1 to detect x_2 is

$$\gamma_{r\to x_2}^{t_2} = \frac{|h_{sr}|^2(1-a)P_t/d_{sr}^{\alpha}}{|h_{sr}|^2 aP_t/d_{sr}^{\alpha} + I_s + N_0}. \tag{6}$$

The SINR of UE1 to decode x_1 is

$$\gamma_{r\to x_1}^{t_2} = \frac{|h_{sr}|^2 aP_t/d_{sr}^{\alpha}}{I_s + N_0}. \tag{7}$$

In this paper, decode-and-forward (DF) is used at UE1 as UE1 should detect x_2 with SIC. Therefore, the received signal of UE2 is

$$y_d(t_2) = \sqrt{P_r}\frac{h_{rd}}{\sqrt{d_{rd}^{\alpha}}}x_2(t_2-\delta)+n_d(t_2), \tag{8}$$

where d_{rd} represents the distance from UE1 to UE2, and n_d is the same as n_r at UE2. Thus, the SINR of UE2 to detect x_2 is

$$\gamma_{d\to x_2}^{t_2} = \frac{P_r|h_{rd}|^2}{d_{rd}^{\alpha}N_0} = \frac{\eta P_t\theta|h_{sr}|^2|h_{rd}|^2}{d_{sr}^{\alpha}d_{rd}^{\alpha}(1-\theta)N_0}. \tag{9}$$

III. OUTAGE PROBABILITY

In this section, we calculate the outage probabilities of UE1 and UE2. Let R_1^t and R_2^t be the required target rates to decode x_1 and x_2, respectively. The required target SINR to decode x_1 and x_2 can be expressed as $\tau_1 = 2^{R_1^t/(1-\theta)}-1$ and $\tau_2 = 2^{R_2^t/(1-\theta)}-1$, respectively.

Proposition 1: If $\tau_2 < \frac{1}{a}-1$, the outage probability of UE1 is written as

$$\mathrm{P}_{out}^{r} = 1-e^{-\lambda_{sr}b_3}. \tag{10}$$

On the other hand, if $\tau_2 \geq \frac{1}{a}-1$, the outage probability of UE1 is one, where

$$\begin{aligned} b_1 &= \frac{(I_s+N_0)d_{sr}^{\alpha}\tau_2}{P_t(1-a-a\tau_2)},\\ b_2 &= \frac{(I_s+N_0)d_{sr}^{\alpha}\tau_1}{aP_t},\\ b_3 &= \max(b_1,b_2). \end{aligned}$$

Proof: The complementary event of the outage at UE1 can be expressed as that UE1 can decode x_2 in the process of SIC and is also able to decode x_1. Thus, the outage probability of UE1 is

$$\begin{aligned} \mathrm{P}_{out}^{r} &= 1-\Pr(\gamma_{r\to x_2}^{t_2}\geq\tau_2, \gamma_{r\to x_1}^{t_2}\geq\tau_1)\\ &\overset{\text{s1}}{=} 1-\Pr(|h_{sr}|^2\geq b_1, |h_{sr}|^2\geq b_2)\\ &= 1-\Pr(|h_{sr}|^2\geq b_3)\\ &= 1-e^{-\lambda_{sr}b_3}, \end{aligned} \tag{11}$$

where equality (s1) holds under the condition of $\tau_2 < \frac{1}{a}-1$; otherwise $\mathrm{P}_{out}^{r}=1$. ■

Proposition 2: If $\tau_2 < \frac{1}{a}-1$, the outage probability of UE2 can be expressed as

$$\mathrm{P}_{out}^{d} \approx 1-\sum_{i=1}^{N_1}\upsilon_i f(t_i). \tag{12}$$

If $\tau_2 \geq \frac{1}{a}-1$, the outage probability of UE2 is one, where

$$\begin{aligned} f(t) &= \lambda_{sr}e^{-[\lambda_{sr}(t+b_1)+\frac{\lambda_{rd}b_4}{t+b1}]}e^{t},\\ \upsilon_i &= \frac{t_i}{(N_1+1)^2[L_{(N_1+1)}(t_i)]^2},\\ L_{N_1}(t) &= \sum_{k=0}^{N_1}\binom{N_1}{k}\frac{(-1)^k}{k!}t^k, \end{aligned}$$

and N_1 is a parameter to achieve an accuracy-complexity tradeoff .

Proof: The complementary event of outage at UE2 can be explained as follows. x_2 can be decoded by UE1 with SIC and it can also be decoded by UE2 itself. Thus, the outage probability of UE2 is

$$\begin{aligned} \mathrm{P}_{out}^{d} &= 1-\Pr(\gamma_{r\to x_2}^{t_2}\geq\tau_2, \gamma_{d\to x_2}^{t_2}\geq\tau_2)\\ &\overset{\text{s2}}{=} 1-\Pr(|h_{sr}|^2\geq b_1, |h_{sr}|^2|h_{rd}|^2\geq b_4)\\ &= 1-\int_{b_1}^{+\infty}\lambda_{sr}e^{-(\lambda_{sr}x+\frac{\lambda_{rd}b_4}{x})}dx, \end{aligned} \tag{13}$$

where $b_4 = \frac{d_{sr}^{\alpha}d_{rd}^{\alpha}(1-\theta)N_0\tau_2}{\eta P_t\theta}$ and equality (s2) holds on the condition that is the same as equality (s1) in Eqn. (11).

It is extremely difficult to calculate the above integral. Thus, we apply Gaussian-Laguerre approximation instead to obtain

$$\mathrm{P}_{out}^{d} \approx 1-\sum_{i=1}^{N_1}\upsilon_i f(t_i). \tag{14}$$

■

Remark 1: From the analytical results, the outage probability of UE1 depends on the required target rates of both UE1 and UE2, but the outage probability of UE2 depends only on its required target rate. Besides, both outage probabilities are inversely proportional to the energy harvested time. Moreover, a larger power allocation coefficient a does not always yield a lower outage probability of UE1.

IV. ERGODIC RATES

In this section, we calculate the ergodic rates of UE1 and UE2, respectively. Let

$$U = \gamma_{r\to x_1}^{t_2} = \frac{|h_{sr}|^2aP_t/d_{sr}^{\alpha}}{I_s+N_0},$$

$$V = \gamma_{r\to x_2}^{t_2} = \frac{|h_{sr}|^2(1-a)P_t/d_{sr}^{\alpha}}{|h_{sr}|^2aP_t/d_{sr}^{\alpha}+I_s+N_0},$$

and

$$W = \gamma_{d\to x_2}^{t_2} = \frac{\eta P_t\theta|h_{sr}|^2|h_{rd}|^2}{d_{sr}^{\alpha}d_{rd}^{\alpha}(1-\theta)N_0}.$$

First, we derive the cumulative distribution functions (CDF) of the above random variables as follows.

$$F_U(u) = 1-e^{-\frac{c_1u}{a}}, \tag{15}$$

$$F_V(v) \overset{\text{s3}}{=} 1-e^{-\frac{c_1v}{(1-a-av)}}, \tag{16}$$

$$F_W(w) = 1-2\sqrt{c_2w}K_1(2\sqrt{c_2w}), \tag{17}$$

where

$$c_1 = \frac{\lambda_{sr}d_{sr}^{\alpha}(I_s+N_0)}{P_t},$$

$$c_2 = \frac{\lambda_{sr}\lambda_{rd}d_{sr}^{\alpha}d_{rd}^{\alpha}(1-\theta)N_0}{\eta\theta P_t},$$

and equality (s3) holds on the condition of $v < \frac{1}{a}-1$; otherwise $F_V(v)=1$.

Proposition 3: The ergodic rate of UE1 can be expressed as

$$R_{e,r} = \frac{(\theta-1)e^{\frac{c_1}{a}}\mathrm{Ei}(-\frac{c_1}{a})}{\ln 2}, \quad (18)$$

where $\mathrm{Ei(x)} = \int_{-\infty}^{x} \frac{e^z}{z}dz$ is an exponential integral function.

Proof: Since x_1 should be decoded only by UE1 itself, the ergodic rate of UE1 is

$$\begin{aligned} R_{e,r} &= (1-\theta)\mathbb{E}\{\left[\log_2(1+\gamma^{t_2}_{r\to x_1})\right]\} \\ &= \frac{(1-\theta)}{\ln 2}\int_0^{+\infty}\frac{1-F_U(u)}{1+u}du \\ &\overset{s4}{=} \frac{(\theta-1)e^{\frac{c_1}{a}}\mathrm{Ei}(-\frac{c_1}{a})}{\ln 2}, \end{aligned} \quad (19)$$

where equality (s4) holds duo to the following relation: $\int_0^{+\infty}\frac{e^{-nx}}{x+m} = -e^{mn}\mathrm{Ei}(-mn)$, with a real number m and $n>0$. ■

Proposition 4: The ergodic rate of UE2 can be expressed as

$$R_{e,r} \approx \frac{c_3(1-\theta)}{\ln 2}\sum_{i=1}^{N_2}\omega_i g(x_i), \quad (20)$$

where

$$g(x) = \frac{2\sqrt{c_2c_3(x+1)^2(1-x)}}{1+c_3(x+1)}e^{\frac{c_1(x+1)}{a(x-1)}}K_1\left[2\sqrt{c_2c_3(x+1)}\right],$$

$$c_3 = \frac{1-a}{2a},$$

and N_2 is the same as N_1, $K_1(x)$ is the first order modified Bessel function of the second kind, $\omega_i = \frac{\pi}{N_2}$, and $x_i = \cos[\frac{(2i-1)\pi}{2N_2}]$.

Proof: Because x_2 should be detected by UE1 with SIC and UE2 itself, the ergodic rate of UE2 is

$$R_{e,d} = (1-\theta)\mathbb{E}\left\{\log_2\left[1+\min(\gamma^{t_2}_{r\to x_2},\gamma^{t_2}_{d\to x_2}\right]\right\}. \quad (21)$$

Let $Z = \min(\gamma^{t_2}_{r\to x_2},\gamma^{t_2}_{d\to x_2})$. The CDF of Z is written as

$$\begin{aligned} F_Z(z) &= \Pr\left[\min(\gamma^{t_2}_{r\to x_2},\gamma^{t_2}_{d\to x_2}) \le z\right] \\ &= 1-\Pr\left(\gamma^{t_2}_{r\to x_2} > z\right)\Pr\left(\gamma^{t_2}_{d\to x_2} > z\right) \\ &= 1-\left[1-F_V(z)\right]\left[1-F_W(z)\right] \\ &= 1-2\sqrt{c_2z}K_1(2\sqrt{c_2z})e^{-\frac{c_1z}{(1-a-az)}}. \end{aligned} \quad (22)$$

Thus, the ergodic rate of UE2 is

$$\begin{aligned} R_{e,d} &= \frac{(1-\theta)}{\ln 2}\int_0^{\frac{1}{a}-1}\frac{1-F_Z(z)}{1+z}dz \\ &= \frac{c_3(1-\theta)}{\ln 2}\int_{-1}^{1}\frac{2\sqrt{c_2c_3(x+1)}}{1+c_3(x+1)} \\ &\quad e^{\frac{c_1(x+1)}{a(x-1)}}K_1\left[2\sqrt{c_2c_3(x+1)}\right]dx. \end{aligned} \quad (23)$$

The above integration is hard to solve. Thus, Gaussian-Chebyshev approximation is used to obtain the result as follows:

$$R_{e,d} \approx \frac{c_3(1-\theta)}{\ln 2}\sum_{i=1}^{N_2}\omega_i g(x_i). \quad (24)$$

■

Remark 2: Obviously, a longer energy harvest time can lower the ergodic rate of UE1, but not always increase the ergodic rate of UE2. In addition, a larger power allocation coefficient a may lead to a larger ergodic rate of UE1 but a smaller ergodic rate of UE2.

V. NUMERICAL RESULTS

The numerical results are illustrated in this section to validate the theoretical analysis on outage probability, ergodic rate, and Jain's fairness. For the sake of fair comparisons, EH-FD-OMA is used as a benchmark, where the BS communicates with UE1 and UE2 in a TDMA manner. Moreover, PS scheme is presented to compare with TS scheme. We set λ_{sr} and λ_{rd} to be 1 and 2. The distances d_{sr} and d_{rd} are set to be 0.5 and 0.25. The path loss exponent α is 4, and noise power N_0 is one. The energy conversion efficiency η is one. The power splitting coefficient β is 0.5. The transmit SNR denotes the ratio of BS transmission power to noise power.

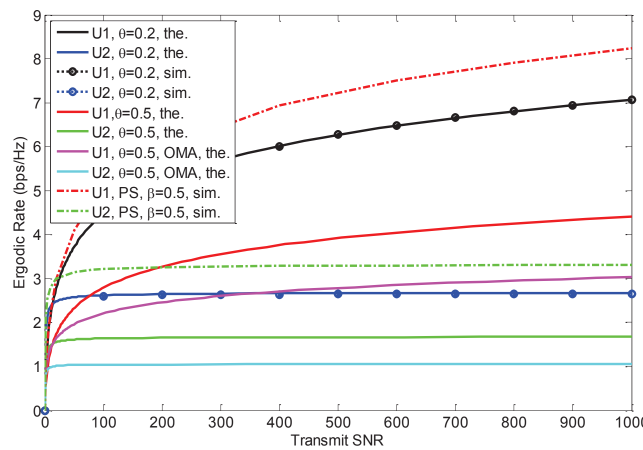

Fig. 2. Ergodic rates versus transmit SNR for UE1 and UE2 with different values of θ.

Fig. 2 shows the impact of θ on the ergodic rates for UE1 and UE2 versus transmit SNR. It is noted that the ergodic rates of UE1 and UE2 increase rapidly in a low transmit SNR region. The ergodic rate of UE2 continues to increase at a low rate, but the ergodic rate of UE1 becomes a constant in a high transmit SNR region. Because the ergodic rate of UE2 is limited by the decoded rate of x_2 at UE1 in the process of SIC. Moreover, it is observed that both of the ergodic rates for UE1 and UE2 increase as θ decreases. Also, it is observed that EH-FD-NOMA outperforms its counterpart EH-FD-OMA.

Fig. 3 depicts the influence of I_s on the outage probabilities for UE1 and UE2 versus transmit SNR. It is observed that the outage probabilities of two users decrease quickly in a low transmit SNR region. Afterwards, both of the outage probabilities of two users tend to be flat over in a high transmit SNR region. In addition, the outage probability increases as self interference power ascends as expected.

Fig. 4 illustrates the Jain fairness index versus transmit SNR with different values of a. Here, the Jain fairness index is defined as $J = \frac{(R_{e,r}+R_{e,d})^2}{2({R_{e,r}}^2+{R_{e,d}}^2)}$. As shown in Fig. 4, the Jain fairness index increases rapidly at a very low transmit

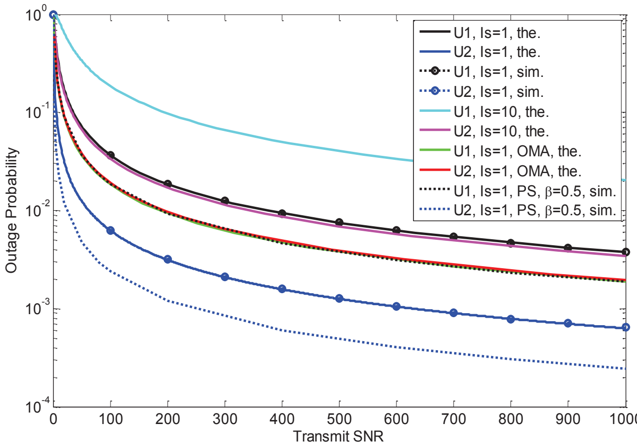

Fig. 3. Outage probability versus transmit SNRs for UE1 and UE2 with different values of I_s.

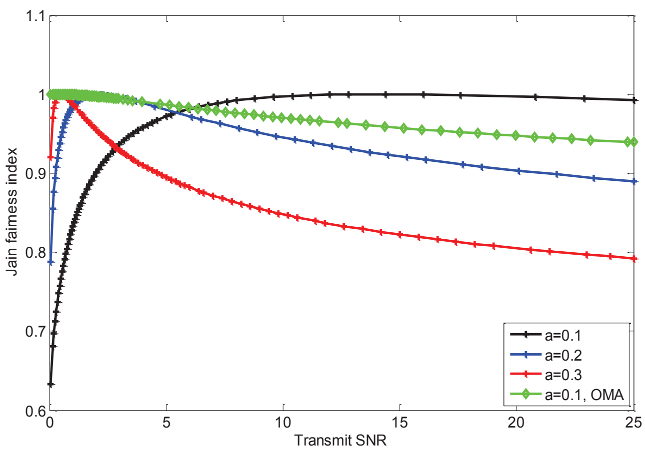

Fig. 4. Jain fairness index versus transmit SNR with different values of a.

SNR. Subsequently, it descends gradually as the transmit SNR increases. Furthermore, a smaller a has its advantage on the fairness in a low transmit SNR region, and a larger a may result in a better fairness in a high transmit SNR region. Also, EH-FD-NOMA has a better performance on the fairness in a high transmit SNR region if compared to EH-FD-OMA.

VI. Conclusion

This paper investigated a cooperative communication scheme, which combines cooperative NOMA, FD relaying, and EH techniques. The closed-form expressions for the outage probabilities and ergodic rates were derived to evaluate the performance of the proposed EH-FD-NOMA system. The theoretical results were verified by the simulation results, showing that the proposed EH-FD-NOMA scheme outperforms its counterparts. We will consider multiple BSs and UEs in our future works.

References

[1] Y. Saito, Y. Kishiyama, A. Benjebbour, T. Nakamura, A. Li, and K. Higuchi, "Non-Orthogonal Multiple Access (NOMA) for Cellular Future Radio Access," 2013 IEEE 77th Vehicular Technology Conference (VTC Spring), Dresden, Germany, pp. 1-5, Jun. 2013.

[2] Z. Ding, M. Peng, and H. V. Poor, "Cooperative Non-Orthogonal Multiple Access in 5G Systems," in IEEE Communications Letters, vol. 19, no. 8, pp. 1462-1465, Aug. 2015.

[3] A. Sabharwal, P. Schniter, D. Guo, D. W. Bliss, S. Rangarajan, and R. Wichman, "In-Band Full-Duplex Wireless: Challenges and Opportunities," in IEEE Journal on Selected Areas in Communications, vol. 32, no. 9, pp. 1637-1652, Sept. 2014.

[4] L. R. Varshney, "Transporting information and energy simultaneously," 2008 IEEE International Symposium on Information Theory, Toronto, pp. 1612-1616, 2008.

[5] X. Zhou, R. Zhang, and C. K. Ho, "Wireless Information and Power Transfer: Architecture Design and Rate-Energy Tradeoff," in IEEE Transactions on Communications, vol. 61, no. 11, pp. 4754-4767, November 2013.

[6] Y. Liu, Z. Ding, M. Elkashlan, and H. V. Poor, "Cooperative Non-orthogonal Multiple Access With Simultaneous Wireless Information and Power Transfer," in IEEE Journal on Selected Areas in Communications, vol. 34, no. 4, pp. 938-953, April 2016.

[7] Y. Xu, C. Shen, Z. Ding, X. Sun, S. Yan, G. Zhu, and Z. Zhong, "Joint Beamforming and Power-Splitting Control in Downlink Cooperative SWIPT NOMA Systems," IEEE Transactions on Signal Processing, vol. 65, no. 18, pp. 4874-4886, Sept. 2017.

[8] Z. Yang, Z. Ding, P. Fan, and N. Al-Dhahir, "The Impact of Power Allocation on Cooperative Non-orthogonal Multiple Access Networks With SWIPT," in IEEE Transactions on Wireless Communications, vol. 16, no. 7, pp. 4332-4343, July 2017.

[9] N. T. Do, D. B. Da Costa, T. Q. Duong, and B. An, "A BNBF User Selection Scheme for NOMA-Based Cooperative Relaying Systems With SWIPT," in IEEE Communications Letters, vol. 21, no. 3, pp. 664-667, March 2017.

[10] Y. Zhang, J. He, S. Guo, and F. Wang, "Energy efficiency maximisation in wireless powered networks with cooperative non-orthogonal multiple access," in IET Communications, vol. 12, no. 18, pp. 2374-2383, Nov. 2018.

[11] T. N. Do, D. B. da Costa, T. Q. Duong, and B. An, "Improving the Performance of Cell-Edge Users in MISO-NOMA Systems Using TAS and SWIPT-Based Cooperative Transmissions," in IEEE Transactions on Green Communications and Networking, vol. 2, no. 1, pp. 49-62, March 2018.

[12] Y. Xu, C. Shen, Z. Ding, X. Sun, S. Yan, and G. Zhu, "Joint beamforming design and power splitting control in cooperative SWIPT NOMA systems," 2017 IEEE International Conference on Communications (ICC), Paris, pp. 1-6, 2017.

[13] Y. Ye, Y. Li, D. Wang, and G. Lu, "Power splitting protocol design for the cooperative NOMA with SWIPT," 2017 IEEE International Conference on Communications (ICC), Paris, pp. 1-5, 2017.

[14] N. T. Do, D. Benevides da Costa, T. Q. Duong, and B. An, "Transmit antenna selection schemes for MISO-NOMA cooperative downlink transmissions with hybrid SWIPT protocol," 2017 IEEE International Conference on Communications (ICC), Paris, pp. 1-6, 2017.

[15] L. Zhang, J. Liu, M. Xiao, G. Wu, Y. Liang and S. Li, "Performance Analysis and Optimization in Downlink NOMA Systems With Cooperative Full-Duplex Relaying," in IEEE Journal on Selected Areas in Communications, vol. 35, no. 10, pp. 2398-2412, Oct. 2017.

[16] M. F. Kader, S. Y. Shin, and V. C. M. Leung, "Full-Duplex Non-Orthogonal Multiple Access in Cooperative Relay Sharing for 5G Systems," in IEEE Transactions on Vehicular Technology, vol. 67, no. 7, pp. 5831-5840, July 2018.

[17] X. Yue, Y. Liu, S. Kang, A. Nallanathan, and Z. Ding, "Exploiting Full/Half-Duplex User Relaying in NOMA Systems," IEEE Transactions on Communications, vol. 66, no. 2, pp. 560-575, Feb. 2018.

[18] Z. Zhang, Z. Ma, M. Xiao, Z. Ding, and P. Fan, "Full-Duplex Device-to-Device-Aided Cooperative Nonorthogonal Multiple Access," IEEE Transactions on Vehicular Technology, vol. 66, no. 5, pp. 4467-4471, May 2017.

[19] T. N. Do, D. Benevides da Costa, T. Q. Duong, and B. An, "A Full-Duplex Cooperative Scheme with Distributed Switch-and-Stay Combining for NOMA Networks," GLOBECOM 2017 - 2017 IEEE Global Communications Conference, Singapore, pp. 1-6, 2017.

[20] Q. Y. Liau, C. Y. Leow, and Z. Ding, "Amplify-and-Forward Virtual Full-Duplex Relaying-Based Cooperative NOMA," IEEE Wireless Communications Letters, vol. 7, no. 3, pp. 464-467, June 2018.

[21] M. Mohammadi, Z. Mobini, H. A. Suraweera, and Z. Ding, "Antenna Selection in Full-Duplex Cooperative NOMA Systems," 2018 IEEE International Conference on Communications (ICC), Kansas City, pp. 1-6, 2018.

[22] X. Yue, Y. Liu, R. Liu, A. Nallanathan, and Z. Ding, "Full/Half-Duplex Relay Selection for Cooperative NOMA Networks," GLOBECOM 2017 - 2017 IEEE Global Communications Conference, Singapore, pp. 1-6, 2017.